

Transfer Process Multiphysics Simulation in Electrophotography¹

T. Sasaki, T. Onishi, A. Sugiyama and S. Nasu
Analysis Technology Center, Canon Inc., Tokyo, Japan
E-mail: sasaki.toyoshige@canon.co.jp

Y. Yoda
Peripherals Development Center, Canon Inc., Shizuoka, Japan

T. Tomizawa
Office Imaging Products Device Development Center, Canon Inc., Ibaraki, Japan

Abstract. The transfer process of color electrophotography involves various materials, including paper, rollers, toner, intermediate transfer belt, and sawlike static charge eliminator. Each component physically interacts with each other, creating electric fields, electric discharges, ion flows, electric conduction, and toner behavior. The authors have developed a numerical simulation method which considers electrical materials, geometric configuration, and physical phenomenon. The method the authors developed was used to calculate current characteristics, electric discharges, and toner scattering in a color electrophotographic system. The results showed good agreement with experiments. Furthermore, the calculation results showed removal of electricity by the static charge eliminator reduces toner scattering and separation discharges. © 2010 Society for Imaging Science and Technology.
[DOI: 10.2352/J.ImagingSci.Technol.2010.54.3.030505]

INTRODUCTION

In electrophotographic systems such as printers or copiers, the intermediate transfer system is commonly used to achieve high quality, high speed, and robust performance. Figure 1(a) shows a schematic diagram of the intermediate transfer system. A toner image on the photoconductor drum is transferred to an intermediate transfer belt (ITB); four monochrome images are transferred from a color image on ITB during the first transfer process. The color image is transferred to paper during the second transfer process. Fig. 1(b) shows the principle of the second transfer process. The ITB is wound around the facing roller whereas the transfer roller is placed on the other side. The paper goes through between the ITB and the transfer roller. The facing roller is kept grounded and a positive voltage is impressed on the transfer roller. The negatively charged toners on the ITB are transferred onto the paper by transfer electric field. The toners are maintained stably on the paper by the positive charge of the paper which is supplied by electric conductivity and static discharges from the trans-

fer roller. A sawlike static charge eliminator is located at the outlet of the nip region. Excess charge on the paper is removed by the ion flow of the static charge eliminator. During the second transfer process, interference from the paper, rollers, toner, ITB, and static charge eliminator may cause electric discharges and toner scattering. Analysis techniques must consider the geometric configuration and multiphysics, which can express the complex interaction of factors: electric discharges across the air gap, ion flows from the static charge eliminator, electric conductivity of materials, and toner motion.

On the other hand, there have been numerous reports on transfer process simulations. One of the traditional ways to calculate a transfer electric field is a one-dimensional electric field calculation,^{1,2} which analyzes a model comprising one-dimensional layers; in other words, the transfer roller, transfer material, air gap, toner, photoreceptor, etc., are all configured along the direction of the diameter of the transfer roller. This model finds each layer of the electrical field when each goes through the nip region assuming electric conductivity based on Ohm's law and discharges based on Paschen's law. However, this method cannot be applied to the second transfer process above, where we expect a complex electrical field because the transfer roller model ignores the electric field in its tangential direction. A new method that can also calculate the electrical conductivity and discharges in two dimensions has been proposed, and it is used in research to

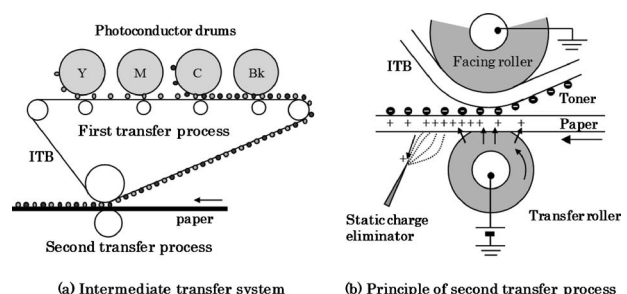


Figure 1. Transfer system of color electrophotography.

¹Presented in part at IS&T's NIP24, Pittsburgh, PA, September 2008.

Received Mar. 25, 2009; accepted for publication Feb. 2, 2010; published online Apr. 15, 2010.

1062-3701/2010/54(3)/030505/8/\$20.00.

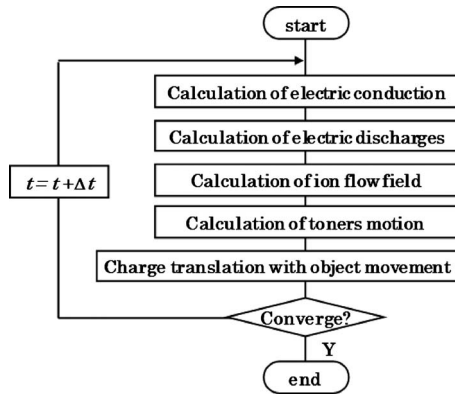


Figure 2. Simulation flowchart.

separate discharge and toner scatter.^{3,4} Nonetheless, in the present work it is difficult to apply this method to a complex model such as the second transfer process because the model calculates the movement of charge caused by discharges using the theory of a parallel plane capacitor. Additionally, since the model is based the finite difference method, it is not easy to calculate a problem that also requires us to consider electrical charge concentration at a needle point, such as on the sawlike static charge eliminator. On the other hand, it has been reported that there is a method that simulates transfer condition of each toner particle in the transfer electrical field using the discrete element method (DEM).^{5,6} There is also a method that can calculate transfer conditions for each toner particle, considering the van der Waals force, the induced image force, the liquid bridge force, the electrostatic force, and even the changes in adhesion brought about by plastic deformation of the toner.⁷ However, these methods require too much time to calculate their DEMs. As a result, the electrical calculation does not reflect the actual charge on a toner particle.

Here, we developed a simulation method that can consider physical phenomena occurring in the second transfer process. This program's functions for electric conductivity and discharges work the same as in the previous version. However, with the aid of the two-dimensional (2D) finite element method (FEM), it has been improved so as also to apply to complex geometric shapes in the second transfer process. Furthermore, the program can consider characteristics of nonlinearity of the material, charge on the toner, and the ion flows transmitted from the static charge eliminator. We have thus developed a numerical simulation method which considers these physical phenomena. This article intends to verify the developed method and to understand control mechanism in the second transfer process.

SIMULATION METHOD

Figure 2 shows the calculation flowchart, which consists of five main calculation steps: electric conductivity, electric discharges, ion flow field, toner motion, and object movement. The details of which are described below.

Electric Conduction

First, we find the electric potential and calculate the movement of charge caused by electrical conduction following the potential distribution that we just found. The potential is expressed with Poisson's equation:

$$\text{div}(\varepsilon \text{grad} \phi) = -\rho, \quad (1)$$

where ε is permittivity, ϕ is potential, and ρ is charge density. We obtain the following equation by limiting ourselves to 2D problems and using the Galerkin method based on FEM:

$$\int \int_{\Omega} \left(\varepsilon \frac{\partial Ni}{\partial x} \frac{\partial \phi}{\partial x} + \varepsilon \frac{\partial Ni}{\partial y} \frac{\partial \phi}{\partial y} \right) dS = \int \int_{\Omega} Ni \rho dS, \quad (2)$$

where Ω is the analysis region and Ni is the interpolating shape function of each element. We solve Eq. (2) and find the potential. Next, we calculate movement of the charge caused by electrical conduction. We use the following equation which considers Ohm's Law, modified by the charge conservation law:

$$\frac{\partial \rho}{\partial t} = \text{div}(\sigma \text{grad} \phi), \quad (3)$$

where σ stands for the electric conductivity. Equation (3) is an equation that replaced " ε " with " σ " and " ρ " with " $-\partial \rho / \partial t$ " from Eq. (1). Hence, Eq. (3) can be expressed as follows:

$$\int \int_{\Omega} Ni \frac{\partial \rho}{\partial t} dS = - \int \int_{\Omega} \left(\sigma \frac{\partial Ni}{\partial x} \frac{\partial \phi}{\partial x} + \sigma \frac{\partial Ni}{\partial y} \frac{\partial \phi}{\partial y} \right) dS. \quad (4)$$

We can find change in charge density based on Ohm's Law from Eq. (4) in this way: we combine Eqs. (2) and (4) and can calculate charge movement. However, in the present work we have used a way to calculate each equation separately in time. The way to calculate time evolution is as follows. First, we calculate electric potential ϕ from Eq. (2); then we add ϕ into Eq. (4). Next we obtain the new charge using the following equation:

$$\int \int_{\Omega} Ni \rho^{(k+1)} dS = \int \int_{\Omega} Ni \rho^{(k)} dS + \int \int_{\Omega} Ni \frac{\partial \rho^{(k)}}{\partial t} \Delta t dS, \quad (5)$$

where $\rho^{(k+1)}$ and $\rho^{(k)}$ represent charge density between the time steps of $k+1$ and k . With the use of the equation above, we can calculate charge movement; however, electric potential after charge has moved has yet been calculated at this point. Thus, we add the values on the left side of Eq. (5) to the right side of Eq. (2) and find the potential after charge moved.

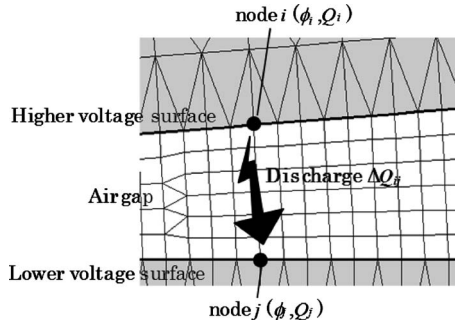


Figure 3. Schematic diagram of electric discharges.

Additionally in Eq. (4), we find the relationship between conductivity σ and electric field by measurement and express the points in a function whereby σ depends on electric field. Then, before calculating Eq. (4), we calculate electric field. After finding conductivity σ that is appropriate for this electric field, we evaluate Eq. (4) using the derived conductivity.

Electric Discharges

We follow Paschen's law regarding the relationship between discharge, starting voltage, and gap length. Figure 3 demonstrates a finite element (FE) model facing two opposite sides. We look for a node that satisfies the condition of Paschen's discharge. The node is found among the nodes on one side that is opposite from the node "i" on the other side. If there is more than one node, we select the one that most exceeds Paschen's voltage. We call it node "j." Also we term these two nodes *discharge node pair* as we assume discharge between them.

We call the charge on nodes i and j before discharge Q_i and Q_j respectively. Also we define Paschen's voltage between those nodes as $V_{pa}^{(ij)}$. We suppose that charge ΔQ_{ij} moves by static discharge, and the potential difference between them will then be at $V_{pa}^{(ij)}$. In this way, the relationship among Q'_i , Q'_j , potential ϕ'_i and ϕ'_j after discharge can be expressed as following:

$$\begin{cases} Q'_i = Q_i - \Delta Q_{ij} \\ Q'_j = Q_j + \Delta Q_{ij} \end{cases} \quad (6)$$

$$\phi'_i - \phi'_j = V_{pa}^{(ij)}. \quad (7)$$

The following equation is designed to introduce electric field into Eq. (2). It is a whole node equation of the FE model:

$$\begin{bmatrix} K_{11} & \cdots & K_{1n} \\ \vdots & \ddots & \vdots \\ K_{n1} & \cdots & K_{nn} \end{bmatrix} \begin{Bmatrix} \phi_1 \\ \vdots \\ \phi_n \end{Bmatrix} = \begin{Bmatrix} Q_1 \\ \vdots \\ Q_n \end{Bmatrix}, \quad (8)$$

where K is a component of the coefficient matrix and n is an unknown node number. By combining Eqs. (6)–(8), we obtain the following:

$$\begin{bmatrix} K_{11} & \cdots & K_{1i} & \cdots & K_{1j} & \cdots & K_{1n} & 0 \\ \vdots & & \vdots & & \vdots & & \vdots & \vdots_0 \\ K_{i1} & \cdots & K_{ii} & \cdots & K_{ij} & \cdots & K_{in} & 1 \\ \vdots & & \vdots & & \vdots & & \vdots & \vdots_0 \\ K_{j1} & \cdots & K_{ji} & \cdots & K_{jj} & \cdots & K_{jn} & -1 \\ \vdots & & \vdots & & \vdots & & \vdots & \vdots_0 \\ K_{n1} & \cdots & K_{ni} & \cdots & K_{nj} & \cdots & K_{nn} & 0 \\ 0 & \cdots & 0 & \cdots & -1 & \cdots & 0 & 0 \end{bmatrix} \begin{Bmatrix} \phi'_1 \\ \vdots \\ \phi'_i \\ \vdots \\ \phi'_j \\ \vdots \\ \phi'_n \\ \Delta Q_{ij} \end{Bmatrix} = \begin{Bmatrix} Q_1 \\ \vdots \\ Q_i \\ \vdots \\ Q_j \\ \vdots \\ Q_n \\ V_{pa}^{(ij)} \end{Bmatrix}. \quad (9)$$

The left matrices consist of 1 and -1 in the discharge node column and contain a row composed of zeroes in other areas and a symmetrical column arrangement. When more than one discharge node pairs exist, columns and rows in addition to n in the matrix increase numerically equivalent to their pair numbers. Since the left matrix is symmetrical, we can solve it in the same way as Eq. (8). This way, we can find discharge charge of each of the discharge nodes. In the process of calculation of the discharged charge, we find each potential ϕ' and Q' from Eqs. (9) and (6).

It is to be noted that the matrix in Eq. (9) contains zero in its diagonal component; hence it requires considerable time to solve by the iteration method. The Appendix provides the method adopted in the actual program to speed up the process.

Discharges to Toner

In the electrical field calculation shown in Eqs. (2) and (9), we considered charge of a toner particle in space by approximating the toner to nearby nodes. For this reason, we have considered the induced image force as well. By finding permittivity as the ratio of the area of the toner to that of each finite element, we also have considered its permittivity.

We show how to calculate discharge toward the toner in Figure 4 when the toner is on the surface. In the process of extracting discharge node pair in the discharge calculation, we did so by defining a node located on the outermost sur-

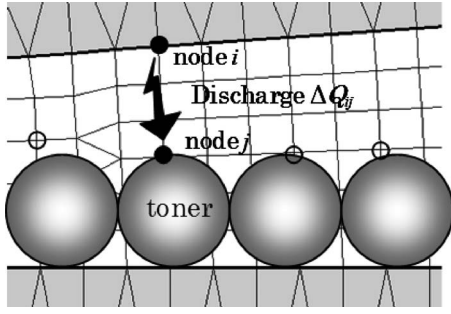


Figure 4. Discharge of toner.

face of the toner layer as the discharge extracting node. During this process, we updated the charge on an individual toner particle by adding the charge ΔQ_{ij} obtained by static discharge to the charge of the toner.

Ion Flow Field

The tip of the sawlike static charge eliminator is where corona discharge arises and ions flow from the tip. The charge transferred from the static charge eliminator is calculated, assuming that the ion flow corresponds to a steady state at each time step. The equation for current continuity is

$$\text{div}(\mu\rho\text{grad}\phi) = 0, \quad (10)$$

where μ is the mobility of air. The following equation is obtained by referring to the vector formula:

$$\mu\text{grad}\phi \cdot \text{grad}\rho = \frac{\mu\rho^2}{\varepsilon_0}, \quad (11)$$

where ε_0 is the permittivity of air. By taking the characteristic lines⁸ into consideration, Eq. (11) can be rewritten as follows:

$$\frac{d\rho}{dt} = -\frac{\mu\rho^2}{\varepsilon_0}, \quad (12)$$

and ρ can be obtained by solving Eq. (12);

$$\rho = \frac{1}{\frac{1}{\rho_0} + \frac{\mu T}{\varepsilon_0}}, \quad (13)$$

where ρ_0 is the electric charge density at the starting point of the ion flow and T is the time for the ions to travel from the starting point to the calculating point in the steady state. We used the value obtained in the experiment for ρ_0 as an origi-

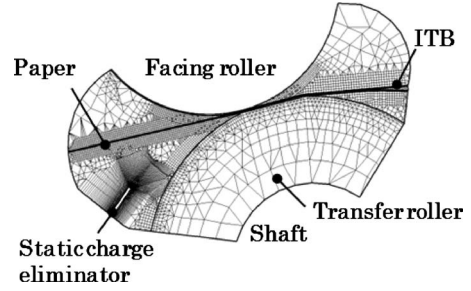


Figure 5. Simulation FE-model for verification.

nal value of charge density on the static charge eliminator. This value is dependent on the electric field at the tip of the static charge eliminator.

Toner Motion

The following equation is written on the assumption that the shape of the toner particle is an ideal sphere and the charge is concentrated at the center;

$$F(t) = Q_T E(t), \quad (14)$$

where F , Q_T , and E are the force on the toner particles, the charge, and the electric field at the center. For calculating the motion of the toner, equations of motion are applied as shown below:

$$\begin{cases} v(t + \Delta t) = v(t) + \frac{F(t)}{m} \Delta t \\ x(t + \Delta t) = x(t) + v(t) \Delta t + \frac{1}{2} \frac{F(t)}{m} \Delta t^2, \end{cases} \quad (15)$$

where v , x , and m are the velocity, location, and weight of the toner particles, respectively. The location of the toner at the next step can be calculated by solving Eq. (15). For collision between toner particles and other objects, the hard sphere collision theory is applied (cf. conservation of momentum).

Furthermore, there are other forces that work on the actual toner such as gravity, air viscosity, and adhesion forces, as well as electrostatic forces. In the calculation below in Eq. (14), we considered only air viscosity for the reason that we want to see the effect of static electricity exclusively.

Object Movement

During the second transfer process, the ITB and paper are transferred as both the transfer roller and the facing roller spin. However, the shape of its surface does not change. For that reason, we express movement of the object as moving charges on its surface in terms of how far it moves at each time step. Additionally, when the electrical conductivity of the object depends on the electric field, the charges inside the object accumulate. So, in this case, we divide it by each element as a layer along the direction of motion of the object, i.e., we move charges along the layer.

Table I. Calculation conditions.

	ϵ'_r	σ (S/m)	Dimensions
Facing roller		∞	$\phi 21$ mm
Transfer roller	61.0	3.2×10^{-8}	$\phi 23$ mm (Shaft = $\phi 12$ mm)
ITB	55.0	Fig. 6	Thickness = $85 \mu\text{m}$
Paper	2.5	2.8×10^{-12}	Thickness = $90 \mu\text{m}$
Toner	2.0	0.0	$\phi 6.8 \mu\text{m}$ (const)

Specific gravity = 1.0 g/cm^3 , $Q/M = -22.4 \mu\text{C/g}$ (const), $M/S = 1.38 \text{ mg/cm}^2$, coefficient of restitution = 0.6, and adhesion/cohesion force = $0[\text{N}]$

RESULTS AND DISCUSSION

The static charge eliminator is located at the outlet of the rollers' nip. It plays an important role in a regular second transfer process. The influence upon electric discharges and the toner motion by the static charge eliminator is discussed below.

Simulation Model

Figure 5 shows the FE model used for verifying the numerical simulation method. This model consists of a facing roller, ITB, transfer roller, paper, and static charge eliminator. The ITB is wound around the facing roller, the paper is in the nip between the ITB and the transfer roller, and the static charge eliminator is kept grounded (GND) and located at the outlet of the nip region. Since the facing roller is already a perfect conductor material, it is not shown in Fig. 5. The facing roller is maintained as GND, and the electric potential (V_T) of the shaft of the transfer roller varies between 1 and 4 kV.

The processing speed is 0.13 m/s . The calculation condition is shown in Table I. The ITBs conductivity has electric field dependence as shown in Figure 6. We defined a calculation time step as $20 \mu\text{s}$. This time step is decided upon the processing speed and the system's time constant. As a result, the paper moves $2.6 \mu\text{m}$ in one time step. Also we defined the smallest measurement for the nip region and the tip of the static charge eliminator elements as $2 \mu\text{m}$ to fully express electric field and discharges. The calculation considers 20,000 steps, which is the period of time that the start of the paper transfers from the furthest right to furthest left. An Intel Xeon 3.8MHz processor is used in this calculation, and approximately 2 h are spent in each calculation. Parallel processing is not applied.

Characteristics

In this system, the currents flow from the shaft of the transfer roller to both the facing roller and the static charge eliminator. Figure 7 shows the calculations and experiments performed to obtain the relationship between V_T and the two

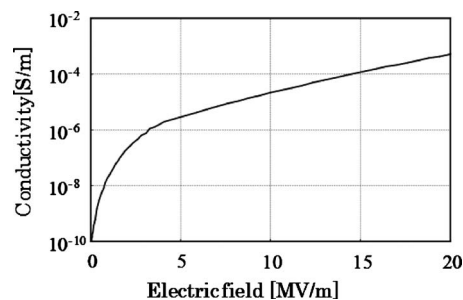


Figure 6. Conductivity curve of ITB.

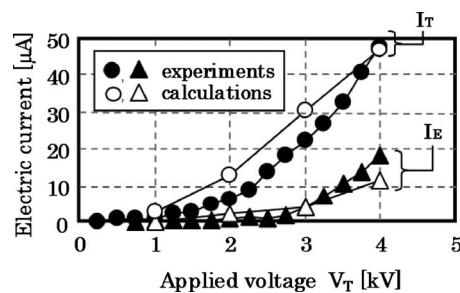


Figure 7. IV characteristics.

currents: one flowing from the shaft of the transfer roller (I_T) and the other flowing to the static charge eliminator (I_E). The results showed that the calculations coincide with experiments in terms of threshold voltage and current increasing rate.

In the IV curves, the experiment shows more nonlinearity than the calculation. Although its cause is not clear, there are several things that could lead this result, such as conductivity of the paper in the nip region where the electric field is extremely large, distribution of roller conductivity in the radial direction, or conductivities on the boundary area of each material.

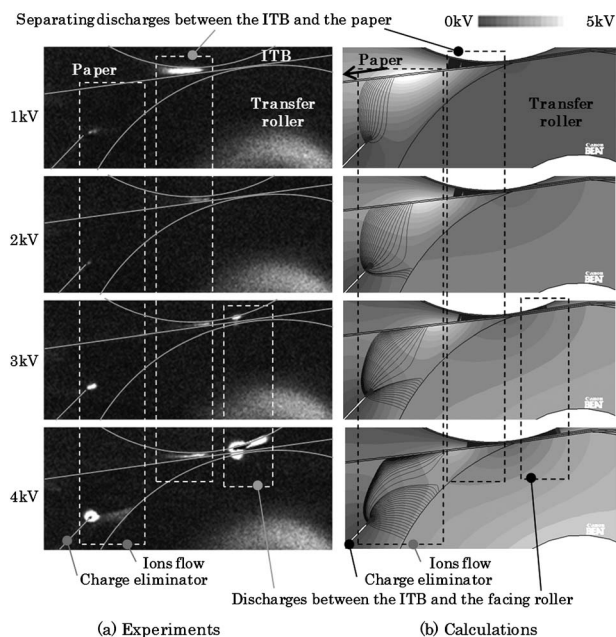


Figure 8. Comparison of electric discharges with experiments and calculations. (a) Experiments: we observed discharge by high sensitivity camera. Object outlines are added as solid lines for ease of viewing. The light regions indicate regions of electrical discharges, but the light region on the transfer roller is noise. (b) Calculations: color shows electric isopotential contour. The black lines emanating from the charge eliminator are ion flow lines.

Electric Discharges

The electric discharge behavior near the outlet of the nip region with the static charge eliminator is shown in Figure 8. Figs. 8(a) and 8(b) are, respectively, experiments and calculations with applied voltage varying from 1 to 4 kV in four

steps. Spark discharge can be seen at the gap between the facing roller and ITB for each voltage. In the calculation, ion flows emanated from the charge eliminator toward paper when voltage was 1 kV. With ascending voltage, the ion flows pour into the transfer roller. On the other hand in the experiment, it is understood that ion flows are emitted from the tip of charge eliminator because the tip of the eliminator appears bright. However, ion flows themselves cannot be seen at 1–3 kV. At 4 kV, ion flows can be seen between the tip of the charge eliminator and the transfer roller as the space between them shimmers slightly.

As for the discharges between the ITB and the facing roller, the calculations and experiments were in accord with discharges starting at 3 kV. Notice that the separation discharges between the ITB and the paper in both the calculations and the experiments reaches the maximum under the 1 kV condition, which is the weakest supply voltage. As can be seen from Fig. 8(b), by supplying a higher voltage, the ion flows expands into the nip region, and charge is removed from around the paper in the nip region. This effect is due to the increase in voltage of the transfer roller and the change in direction of the electric field near the tip of the eliminator, from the paper toward the nip region. By supplying a higher voltage, the eliminator removes the charge on the paper at the nip region. As a result, the discharges between the paper and ITB decrease.

Toner Scattering

Figure 9 shows the condition of layers of the toner. Experiments are at a point far from the nip, and calculations are at a point about 6 mm down from the nip. The calculations qualitatively agree with the experiments in the following respects: the toner at $V_T=2$ kV without the eliminator com-

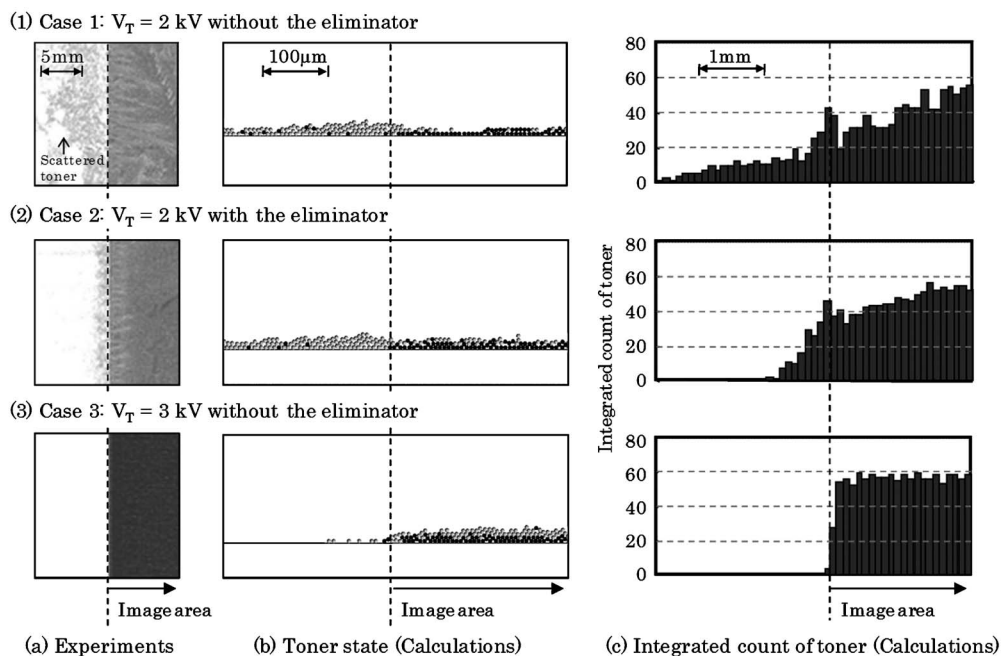


Figure 9. Toner scattering. Experimental results show transferred toner image on paper.

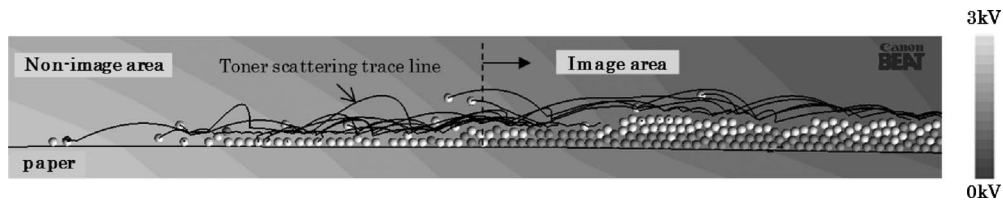


Figure 10. Trajectory of scattering toner (case 1: $V_T=2$ kV without eliminator).

pletely scatters (case 1), the toner at $V_T=2$ kV with the eliminator still scatters but at a reduced rate (case 2), and the toner at $V_T=3$ kV has almost no scattering despite the absence of the eliminator (case 3).

Figure 10 shows the trajectory of toner scattering for case 1. In this figure, the contour illustrates the distribution of electric potential, and the black lines trace the scattering toner. It is clear from this figure that the electric potential gradient from the image area to nonimage area is the cause of scattering toner. The reason for changes in toner scattering behavior moving from case 1 to case 3 is as follows.

Figures 11 and 12 show the calculated results for electric field variation. Toners are kept at the same spot to prevent from being scattered on the paper while the paper is being transported, which verifies the kind of force that acts on the toners. Figure 11 shows the charge density, which is the sum of paper charge and toner charge. Figure 12 shows the electric potential contour around the boundary region of image and nonimage areas. The black lines in Fig. 12 (2) represent ion flows from the static charge eliminator. When applying 2 kV (case 1), there is not enough positive charge on the paper in the image area to neutralize the negative charge from the toner. Thus, the voltage on the image area is lower than that on the nonimage area. Consequently, the toner on the image area scatters over the nonimage area. However, a static charge eliminator added to this system (case 2) will neutralize the positive charge on the nonimage area, and the electric potential gradient from the image area to the nonimage area will weaken, thus reducing the scattering. In addition, by shifting the voltage to 3 kV (case 3), the paper in the image area will have enough positive charge to attract the negative charged toner, and scattering will not occur even without the eliminator.

CONCLUSION

A numerical simulation method for the transfer process in an electrophotographic system, which takes into consideration electric discharges, ion flows, charge conduction, and toner behavior, was developed. The method was applied to the analysis of the second transfer (belt to paper) process. The results showed good qualitative agreement with experiments. It was found that ion flows from the static charge eliminator affect the behavior of separation discharges and toner scattering.

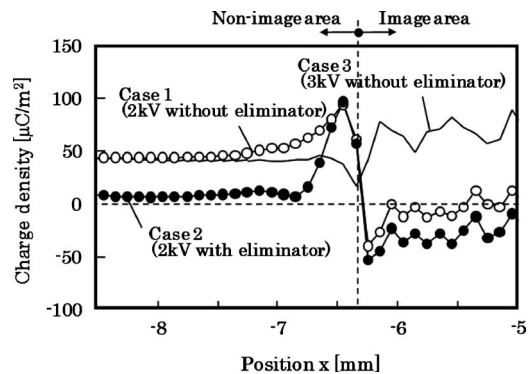


Figure 11. Distribution of charge density for the sum of paper charge and toners charge.

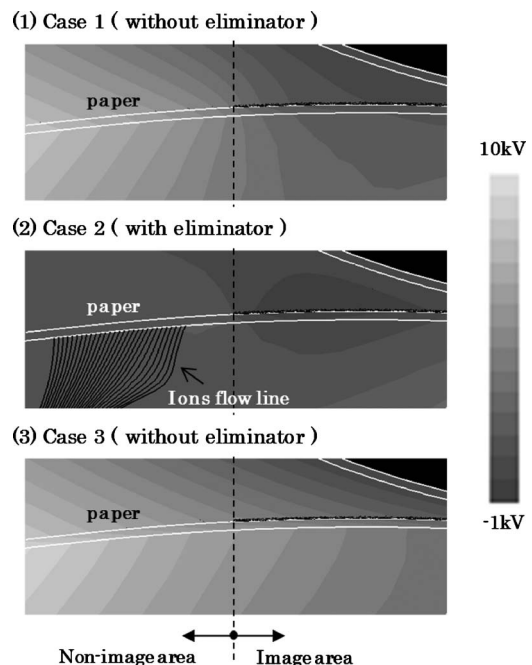


Figure 12. Electric potential at the outlet of the nipped region.

APPENDIX: HOW TO SOLVE THE DISCHARGE CALCULATION MATRIX

Put Eqs. (6) and (7) into Eq. (8) and obtain the following:

$$\begin{bmatrix} K_{11} & & & & & \\ \vdots & \ddots & & & & \\ K_{i1} & \cdots & K_{ii} & & & \\ \vdots & \ddots & \vdots & \ddots & & \\ K_{j1} & \cdots & K_{ji} & \cdots & K_{jj} & \\ \vdots & \ddots & \vdots & \ddots & \vdots & \ddots \\ K_{n1} & \cdots & K_{ni} & \cdots & K_{nj} & \cdots & K_{nn} \end{bmatrix} \begin{Bmatrix} \phi'_1 \\ \vdots \\ \phi'_j + V_{pa}^{(ij)} \\ \vdots \\ \phi'_j \\ \vdots \\ \phi'_n \end{Bmatrix} = \begin{Bmatrix} Q_1 \\ \vdots \\ Q_i - \Delta Q_{ij} \\ \vdots \\ Q_j + \Delta Q_{ij} \\ \vdots \\ Q_n \end{Bmatrix}. \quad (A1)$$

Then rearrange to obtain the following:

$$\begin{bmatrix} K_{11} & & & & & \\ \vdots & \ddots & & & & \\ K_{i1} & \cdots & K_{ii} & & & \\ \vdots & \ddots & \vdots & \ddots & & \\ K_{j1} & \cdots & K_{ji} & \cdots & K_{jj} & \\ \vdots & \ddots & \vdots & \ddots & \vdots & \ddots \\ K_{n1} & \cdots & K_{ni} & \cdots & K_{nj} & \cdots & K_{nn} \end{bmatrix} \begin{Bmatrix} \phi'_1 \\ \vdots \\ \phi'_j \\ \vdots \\ \phi'_j \\ \vdots \\ \phi'_n \end{Bmatrix} = \begin{Bmatrix} Q_1 \\ \vdots \\ Q_i - \Delta Q_{ij} \\ \vdots \\ Q_j + \Delta Q_{ij} \\ \vdots \\ Q_n \end{Bmatrix} - [K] \begin{Bmatrix} 0 \\ \vdots \\ V_{pa}^{(ij)} \\ \vdots \\ 0 \\ \vdots \\ 0 \end{Bmatrix}. \quad (A2)$$

Supposing the second term of the right-hand member is {R}, we can reorganize the equation further and obtain the following:

$$\begin{bmatrix} K_{11} & & & & & \\ \vdots & \ddots & & & & \\ K_{i1} + K_{j1} & \cdots & K_{ii} + K_{ij} + K_{ji} + K_{jj} & & & \\ \vdots & \ddots & \vdots & \ddots & & \\ K_{n1} & \cdots & K_{ni} + K_{nj} & \cdots & K_{nn} & \end{bmatrix} \begin{Bmatrix} \phi'_1 \\ \vdots \\ \phi'_j \\ \vdots \\ \phi'_n \end{Bmatrix} = \begin{Bmatrix} Q_1 \\ \vdots \\ Q_i + Q_j \\ \vdots \\ Q_n \end{Bmatrix} - \begin{Bmatrix} R_1 \\ \vdots \\ R_i + R_j \\ \vdots \\ R_n \end{Bmatrix}. \quad (A3)$$

This equation does not include zero in the diagonal elements. Solving this equation we find {ϕ'} and substitute it into Eq. (A1) which gives us $Q_i - \Delta Q$ and $Q_j + \Delta Q$. Since Q_i and Q_j are the charges on nodes i and j , respectively, they are already known. Thus, we can find ΔQ .

REFERENCES

- ¹M. C. Zaretsky, "Performance of an electrically biased transfer roller in a Kodak ColorEdge™ CD copier", *J. Imaging Sci. Technol.* **37**, 187–191 (1993).
- ²T. Ito and H. Kawamoto, "Numerical simulation of biased roller transfer by one-dimensional quasisteady electric field", *Int. J. Appl. Electromagn. Mech.* **13**, 85–92 (2001/2002).
- ³M. Kadonaga, "Two-dimensional electrical simulation of charging roller in electrophotography", *J. Imaging Soc. of Jpn.* **38**, 97–102 (1999) (in Japanese).
- ⁴M. Kadonaga, T. Katoh, T. Takahashi, and Y. Kishi, "Numerical simulation of separating discharge in the belt transfer system", *J. Imaging Sci. Technol.* **45**, 547–555 (2001).
- ⁵M. Kadonaga, T. Takahashi, and H. Iimura, "Numerical simulation of toner movement in a transfer process", *Proc. IS&T's NIP21* (IS&T, Springfield, VA, 2005) pp. 594–596.
- ⁶S. Aoki, M. Sukesako, and M. Kadonaga, "A numerical simulation method of toner transfer considering voltage distribution of transfer belt", *Proc. IS&T's NIP23* (IS&T, Springfield, VA, 2007) pp. 77–80.
- ⁷N. Nakayama and H. Mukai, "Numerical simulation of electrostatic transfer process using discrete element method", *Proc. Japan Hardcopy 1998* (ISJ, Tokyo, 1998) pp. 261–264.
- ⁸J. L. Davis and J. F. Hoburg, "HVDC transmission line computations using finite element and characteristics methods", *J. Electrostat.* **18**, 1–22 (1986).